6358 *Biochemistry* **2010,** *49,* 6358–6364
DOI: 10.1021/bi100773g

BIOCHEMISTRY
including biophysical chemistry & molecular biology
Article

Mechanistic Investigation of the Inhibition of Aβ42 Assembly and Neurotoxicity by Aβ42 C-Terminal Fragments[†]

Huiyuan Li,[‡] Bernhard H. Monien,[‡,●] Aleksey Lomakin,[@] Reeve Zemel,[‡] Erica A. Fradinger,[‡,○] Miao Tan,[§] Sean M. Spring,[‡] Brigita Urbanc,[▽] Cui-Wei Xie,[§,∥] George B. Benedek,[@,#] and Gal Bitan*[,‡,∥,⊥]

[‡]*Department of Neurology, David Geffen School of Medicine,* [§]*Department of Psychiatry and Biobehavioral Sciences, David Geffen School of Medicine,* [∥]*Brain Research Institute,* [⊥]*Molecular Biology Institute, University of California, Los Angeles, California 90095,* [@]*Materials Processing Center, and* [#]*Department of Physics, Massachusetts Institute of Technology, Cambridge, Massachusetts 02142, and* [▽]*Physics Department, Drexel University, Philadelphia, Pennsylvania 19104.* [●]*Current address: Deutsches Institut für Ernährungsforschung Potsdam-Rehbrücke, Abt. Ernährungstoxikologie, Arthur-Scheunert-Allee 114-116, 14558 Nuthetal, Germany.* [○]*Current address: Department of Biology, Whittier College, 13406 E. Philadelphia St., Whittier, CA 90608.*

Received May 17, 2010; Revised Manuscript Received June 18, 2010

ABSTRACT: Oligomeric forms of amyloid β-protein (Aβ) are key neurotoxins in Alzheimer's disease (AD). Previously, we found that C-terminal fragments (CTFs) of Aβ42 interfered with assembly of full-length Aβ42 and inhibited Aβ42-induced toxicity. To decipher the mechanism(s) by which CTFs affect Aβ42 assembly and neurotoxicity, here, we investigated the interaction between Aβ42 and CTFs using photoinduced cross-linking and dynamic light scattering. The results demonstrate that distinct parameters control CTF inhibition of Aβ42 assembly and Aβ42-induced toxicity. Inhibition of Aβ42-induced toxicity was found to correlate with stabilization of oligomers with a hydrodynamic radius (R_H) of 8−12 nm and attenuation of formation of oligomers with an R_H of 20−60 nm. In contrast, inhibition of Aβ42 paranucleus formation correlated with CTF solubility and the degree to which CTFs formed amyloid fibrils themselves but did not correlate with inhibition of Aβ42-induced toxicity. Our findings provide important insight into the mechanisms by which different CTFs inhibit the toxic effect of Aβ42 and suggest that stabilization of nontoxic Aβ42 oligomers is a promising strategy for designing inhibitors of Aβ42 neurotoxicity.

Alzheimer's disease (AD)[1] is the most common neurodegenerative disease, affecting more than 35 million people worldwide (*1*). Abundant evidence suggests that oligomeric forms of amyloid β-protein (Aβ) are the main neurotoxins causing AD (*2*, *3*). Two main forms of Aβ exist in vivo, containing 40 (Aβ40) or 42 (Aβ42) amino acid residues. Aβ42 plays a central role in the pathogenesis of AD (*4*, *5*). Compared to Aβ40, Aβ42 is substantially more toxic, forms higher-order oligomers, and follows a different oligomerization pathway (*6*, *7*). Peptide inhibitors of Aβ assembly and neurotoxicity reported previously mainly targeted Aβ fibril formation (*8*). The sequences of such inhibitors were based on random selection (*9*), self-recognition of the central hydrophobic cluster (CHC) of Aβ (*10*−*13*), or structural modifications of sequences from the CHC or C-terminal regions (*14*−*17*). As the hypothesis of the cause of AD shifted from Aβ fibril formation and deposition to oligomeric Aβ, the design strategy for peptide inhibitors for treatment of AD was adjusted to target Aβ oligomerization. In view of the important role of the C-terminus in Aβ42 assembly and toxicity, we hypothesized that the C-terminal fragments (CTFs) of Aβ42 might disrupt Aβ42 assembly and inhibit its neurotoxicity. In a previous study, we confirmed this hypothesis and found that Aβ42 CTFs [Aβ(x−42), x = 28−39], with the exception of Aβ(28−42), inhibited Aβ42-induced neurotoxicity (*18*). Among these CTFs, Aβ(31−42) and Aβ(39−42) displayed outstanding inhibitory effects. In addition to inhibiting Aβ42-induced neuronal death, these CTFs were found to rescue disruption of synaptic activity by Aβ42 oligomers at micromolar concentrations (*18*). Initial biophysical assessment suggested that these two CTFs exerted their inhibitory activity via distinct mechanisms (*18*). However, to gain further mechanistic insight, additional investigation of the characteristics of the CTFs themselves, and of their interaction with Aβ42, including comparison of Aβ(31−42) and Aβ(39−42) to other CTFs with low or high activity, was necessary.

Recently, we reported a systematic characterization of biophysical properties of all the CTFs in the original series (*19*), to which we added for additional structural insight two Aβ40 CTFs, Aβ(34−40) and Aβ(30−40), and a fragment derived from the putative folding nucleus of Aβ, Aβ(21−30) (*20*). We found that most of Aβ42 CTFs longer than eight residues readily formed β-sheet-rich fibrils, whereas the shorter CTFs did not. The two Aβ40 CTFs were substantially less prone to aggregation than their Aβ42 CTF counterparts (*19*). Surprisingly, Aβ(30−40) was found to be a strong inhibitor of Aβ42-induced toxicity. Importantly, we found that the capability of the CTFs to inhibit

[†]The work was supported by Grants AG027818 from National Institute on Aging and 2005/2E from the Larry L. Hillblom Foundation.

*To whom correspondence should be addressed: Department of Neurology, David Geffen School of Medicine, University of California at Los Angeles, Neuroscience Research Building 1, Room 451, 635 Charles E. Young Dr. S., Los Angeles, CA 90095-7334. E-mail: gbitan@mednet.ucla.edu. Telephone: (310) 206-2082. Fax: (310) 206-1700.

[1]Abbreviations: AAA, amino acid analysis; Aβ, amyloid β-protein; AD, Alzheimer's disease; CHC, central hydrophobic cluster; CTF, C-terminal fragment; DLS, dynamic light scattering; LDH, lactate dehydrogenase; LMW, low molecular weight; mEPSC, miniature excitatory postsynaptic currents; MWCO, molecular weight cutoff filter; PICUP, photoinduced cross-linking of unmodified proteins.

 Published on Web 06/22/2010

Table 1: Peptide Sequences

Peptide	Sequence
Aβ(39–42)	VVIA
Aβ(38–42)	GVVIA
Aβ(37–42)	GGVVIA
Aβ(36–42)	VGGVVIA
Aβ(35–42)	MVGGVVIA
Aβ(34–42)	LMVGGVVIA
Aβ(33–42)	GLMVGGVVIA
Aβ(32–42)	IGLMVGGVVIA
Aβ(31–42)	IIGLMVGGVVIA
Aβ(30–42)	AIIGLMVGGVVIA
Aβ(29–42)	GAIIGLMVGGVVIA
Aβ(28–42)	KGAIIGLMVGGVVIA
Aβ(34–40)	LMVGGVV
Aβ(30–40)	AIIGLMVGGVV
Aβ(21–30)	AEDVGSNKGA

Aβ42 toxicity did not correlate with their propensity to aggregate or form β-sheet-rich amyloid structures. Rather, inhibition of toxicity appeared to correlate with a coil−turn structure identified by molecular dynamics simulations using experimental ion mobility spectrometry−mass spectrometry data as structural constraints (*21*).

To improve our understanding of the mechanism(s) by which CTFs inhibit Aβ42-induced toxicity, we asked whether they inhibited Aβ42 assembly and, if so, to what extent inhibition of Aβ42 assembly correlated with inhibition of Aβ42-induced toxicity. Here we used photoinduced cross-linking of unmodified proteins (PICUP) and dynamic light scattering (DLS) to study Aβ42 assembly in the absence or presence of CTFs and control peptides and correlated the findings with our previously published data on inhibition of Aβ42 toxicity. The sequences of all the peptides used are listed in Table 1.

MATERIALS AND METHODS

Peptide Preparation. Aβ42, CTFs, and control peptides were synthesized by solid-phase techniques (*22*), using 9-fluorenylmethoxycarbonyl (FMOC) chemistry, as described previously (*19*, *23*, *24*), purified by high-performance liquid chromatography and analyzed by mass spectrometry and amino acid analysis (AAA).

Cell Viability Assays. Previously, a cell viability screen showed that all Aβ42 CTFs, except Aβ(28−42), which was highly toxic itself, inhibited Aβ42-induced toxicity (*18*). Under similar conditions, Aβ(30−40) exhibited strong inhibitory activity, whereas Aβ(34−40) and Aβ(21−30) were inactive (*19*). Here we used lactate dehydrogenase (LDH) experiments to evaluate the inhibition of Aβ(30−40) dose-dependently. The method was described previously (*18*). Briefly, Aβ42/Aβ(30−40) mixtures with concentration ratios of 1:0, 1:1, 1:2, 1:5, and 1:10 were added to the differentiated rat pheochromocytoma (PC-12) cells and incubated for 48 h. Cell death was assessed by the CytoTox-ONE Homogenous Membrane Integrity Assay (LDH assay, Promega, Madison, WI). Three independent experiments with six replicates (n = 18) were conducted, and the results were averaged and presented as mean ± the standard error of the mean.

Electrophysiological Studies. Spontaneous miniature excitatory postsynaptic currents (mEPSCs) of mouse primary hippocampal neurons in the presence of Aβ42 and in the absence or presence of Aβ(31−42) or Aβ(39−42) were reported previously (*18*). Here we used the same method to measure Aβ42 in the presence of Aβ(30−40). Briefly, cells were perfused at a flow rate of 0.4−0.5 mL/min with peptide samples of 3 μM Aβ42 and the Aβ42/Aβ(30−40) mixture at a 1:10 concentration ratio, or vehicle control (extracellular solution with a volume of DMSO equal to that used to dissolve the peptide). To calculate the mEPSC amplitude and frequency, events were analyzed for 1 min before and every 5 min during the application of peptide samples. mEPSC frequency data are presented as mean ± the standard error of the mean.

Photoinduced Cross-Linking of Unmodified Proteins (*PICUP*). PICUP experiments for Aβ(31−42) and Aβ(39−42) were described previously (*18*). Here we expanded these experiments to the entire series of Aβ42 CTFs, the two Aβ40 CTFs, and Aβ(21−30). Briefly, peptides were dissolved in 60 mM NaOH and diluted with 10 mM sodium phosphate (pH 7.4). Low-molecular weight (LMW) Aβ42 was prepared by filtration through a 10000 molecular weight cutoff filter (MWCO) (*25*) or by centrifugation at 16000*g* for 10 min (because some batches of Aβ42 had low solubility and yielded an insufficient concentration for PICUP experiments). Solutions of Aβ fragments were sonicated for 1 min and then filtered through an Anotop 10 syringe filter with a 20 nm pore size (Whatman, Florham Park, NJ). The final concentration of each peptide was determined by AAA. The solution of LMW Aβ42 was mixed with different nominal concentrations of Aβ fragments, and the mixtures were cross-linked immediately, fractionated by SDS−PAGE, silver stained, and subjected to densitometric analysis using ONE-Dscan (Scanalytics, Fairfax, VA). Three replicates were measured for each peptide. The abundance of the Aβ42 hexamer was normalized to the entire lane and reported as mean ± the standard error of the mean. IC_{50} values were calculated by fitting of hexamer abundance versus the logarithm of CTF concentration using Prism (GraphPad, La Jolla, CA).

Dynamic Light Scattering (*DLS*). Solutions of Aβ42 in the absence or presence of CTFs were measured using an in-house-built optical system with a He−Ne laser (wavelength of 633 nm, power of 50 mW) (Coherent, Santa Clara, CA) as a light source and using either PD2000DLS or multitau PD4047 Precision Detectors correlators. The size distribution of scattering particles was reconstructed from the scattered light correlation function using PrecisionDeconvolve (Precision Detectors, Bellingham, MA) based on the regularization method of Tikhonov and Arsenin (*26*).

Peptides were prepared at the University of California by dissolution in 60 mM NaOH and diluted with 10 mM sodium phosphate (pH 7.4). Aβ42/CTF mixtures (30 μM each) contained Aβ42 and Aβ(x−42), where x = 29, 30, 31, 32, 35, or 39, or Aβ(30−40). For transportation from the University of California to the Massachusetts Institute of Technology for measurements, 200 μL samples were lyophilized, stored at −20 °C, and shipped. The samples then were reconstituted in 200 μL of water. The solutions were sonicated for 1 min and filtered through an Anotop 10 syringe filter (20 nm pore size) prior to DLS measurements. The hydrodynamic radius and intensity of particles were recorded. The particle growth rate (dR_H/dt), i.e., the increase in the hydrodynamic radius over time, was determined using at least 20 measurements of 10 min each taken immediately after sample preparation and no less than 10 measurements taken on the next day. The data are presented as mean ± the standard error of the mean. Three replicates were measured for each peptide.

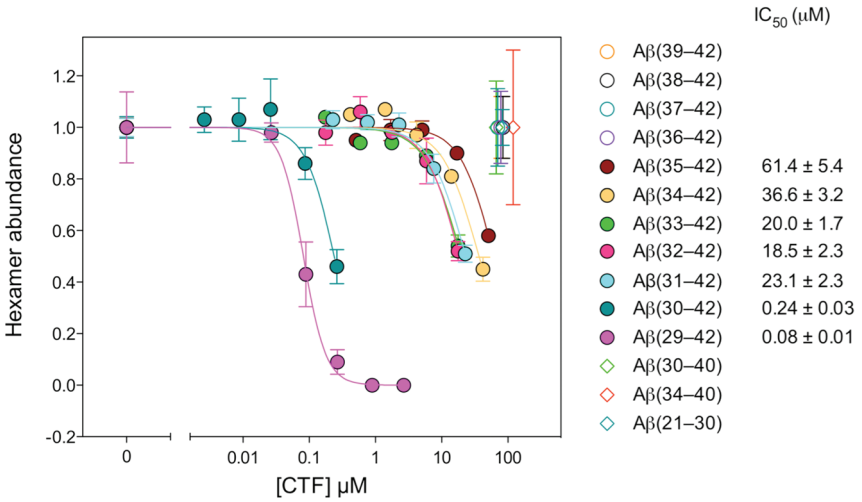

FIGURE 1: Inhibition of Aβ42 hexamer formation. Aβ42 was cross-linked in the absence or presence of increasing concentrations of each CTF and analyzed by SDS−PAGE and silver staining. The amount of Aβ42 hexamer was determined densitometrically and normalized to the protein content in the entire lane. IC_{50} values are the CTF concentrations required for 50% inhibition of Aβ42 hexamer formation.

RESULTS

Aβ42 Oligomerization in the Presence of CTFs. Previously, using PICUP (*27*), the oligomer size distribution of Aβ42 was found to contain abundant pentamers and hexamers, which were termed "paranuclei" (*6*). The abundance of these paranuclei, particularly the hexamers, was found to be a sensitive probe for testing inhibition of Aβ42 oligomerization (*28*). Importantly, because all Aβ fragments used here contained only residues that have low reactivity in PICUP chemistry (*18*, *28*), cross-linking of CTFs to Aβ42 or to themselves was not observed, facilitating unhindered analysis of Aβ42 oligomer size distributions. LMW Aβ42 was prepared by filtration through a 10000 MWCO (*25*) at ~30 μM, mixed with increasing concentrations of each peptide, and cross-linked. The cross-linked mixtures were analyzed by SDS−PAGE and densitometry. Examples are shown in Figure S1 of the Supporting Information.

Previously, we found that Aβ(31−42) inhibited Aβ42 hexamer formation dose-dependently, whereas Aβ(39−42) did not (*18*). Here, all other Aβ42 CTFs, Aβ40 CTFs, and Aβ(21−30) were tested. Analysis of densitometric data showed that Aβ(36−42) and shorter Aβ42 CTFs at concentrations above 100 μM did not inhibit Aβ42 hexamer formation (Figure S1C). Similarly, Aβ40 CTFs and Aβ(21−30) had no effect on Aβ42 hexamer formation (Figure 1). In contrast, Aβ(35−42) and longer Aβ42 CTFs caused a dose-dependent decrease in Aβ42 hexamer abundance (Figure 1 and Figure S1A,B). The inhibitory activity increased with peptide length from Aβ(35−42) through Aβ(33−42), whereas additional elongation to Aβ(32−42) and Aβ(31−42) had little effect on activity. Remarkably, further elongation to Aβ(30−42) and Aβ(29−42) resulted in increases in inhibitory activity of ~2 orders of magnitude, yielding nanomolar IC_{50} values.

Aβ42 Particle Growth in the Presence of CTFs. To further evaluate the interaction between CTFs and Aβ42, we used DLS. PICUP and DLS are complementary methods for investigation of Aβ assembly. PICUP offers high-resolution detection of low-order oligomers, whereas DLS enables noninvasive detection of high-order assemblies with high sensitivity (*6*, *29*). Of the 12 Aβ42 CTFs, we selected six for DLS characterization of their interactions with full-length Aβ42. Aβ(30−42), Aβ(31−42), and Aβ(39−42) were studied because they were the strongest inhibitors of Aβ42-induced neurotoxicity (*18*). Aβ(29−42) was included as the most potent inhibitor of Aβ42 hexamer formation (Figure 1). Aβ(32−42) was selected because it stood out in the CTF series. This CTF was slightly toxic itself, was less efficient than Aβ(31−42) or Aβ(33−42) as an inhibitor of Aβ42-induced toxicity, and displayed unusual aggregation behavior, namely forming predominantly amorphous, rather than fibrillar, aggregates (*19*). Aβ(35−42) was selected as a negative control with relatively low inhibitory activity in both the toxicity (*18*) and oligomerization (Figure 1) assays. Finally, Aβ(30−40) was studied as a potent (IC_{50} = 29 ± 4 μM in the LDH assay) Aβ40-derived inhibitor of Aβ42-induced neurotoxicity (Figure S2 of the Supporting Information).

Similar to previous observations (*6*), in the absence of CTFs, immediately after preparation, Aβ42 comprised predominantly two populations of particles: particles with a hydrodynamic radius R_{H1} of 8−12 nm, which remained largely unchanged during the measurements, and particles with an R_{H2} of 20−60 nm, which were observed in some measurements and tended to fluctuate substantially. We name these oligomer populations P_1 and P_2, respectively. Note that the large oligomers comprising the P_2 fraction cannot possibly pass through a 20 nm pore size filter and therefore must form immediately after filtration. After several days, large particles, presumably fibrils, formed (Figure 2, bottom). The long CTFs themselves, e.g., Aβ(29−42), Aβ(30−42), Aβ(31−42), and Aβ(30−40), exhibited aggregation in DLS measurements (*19*). However, because in the equimolar mixtures of CTF and Aβ42 used here the CTF mass is several times lower than that of Aβ42, the contribution of CTFs alone to the observed scattering is negligible.

In the presence of the seven CTFs we tested, immediately after preparation, a significant enrichment of population P_2 was observed (Figure 2, first column). It is important to consider, however, that the scattering intensity is proportional to the square of the average mass of particles in each fraction. Thus, although the relative contribution of P_2 particles to the observed scattering was large, their weight fraction in the Aβ42/CTF mixtures was still no more than a few percent. During the experiments, the size of P_1 remained relatively unchanged, whereas P_2 appeared to grow in size. Notably, substantial differences in the P_2 growth rate, dR_{H2}/dt, were observed in the presence of different CTFs (Figure 3A). In fact, the strongest toxicity inhibitor,

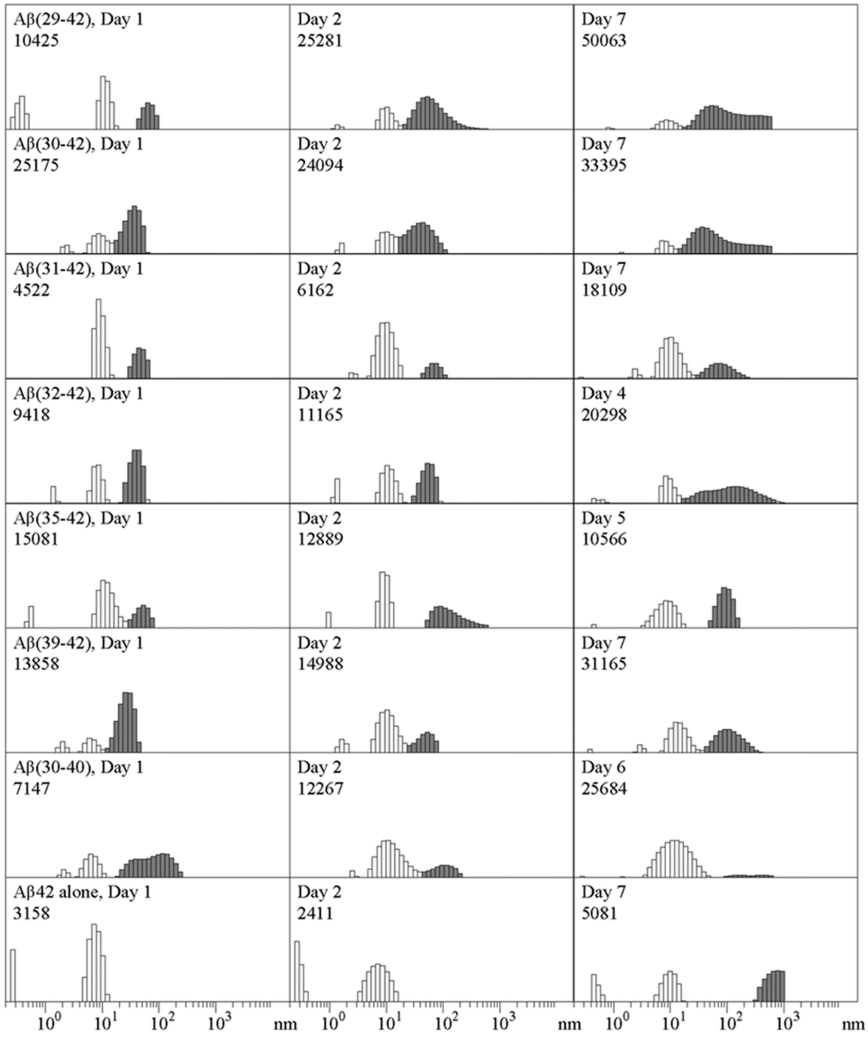

FIGURE 2: CTF effect on Aβ42 particle size distribution. Representative distributions of Aβ42 in the absence or presence of CTFs immediately after preparation (left), on the next day (center), and after 4−7 days (right). White bars represent data for P_1 particles. Gray bars represent data for P_2 or larger particles (in the case of Aβ42 alone). Days of measurement and the total scattering intensities in counts per second are shown in the top left corner of each panel. Only intensities within the same row are directly comparable with each other.

Aβ(31−42), decreased dR_{H2}/dt substantially by 60 ± 13% relative to that of Aβ42 alone. Aβ(39−42) had a weaker effect on dR_{H2}/dt, decreasing the rate by 35 ± 28%. Other CTFs had little or no effect.

Interestingly, on day 1, smaller R_H values were observed in the presence of Aβ(39−42) (R_{H1} = 6 ± 3 nm, and R_{H2} = 30 ± 10 nm) relative to those with other CTFs (Figure 2). Similarly, in the presence of Aβ(30−40), P_1 particles had an R_{H1} of 6 ± 3 nm on day 1, though P_2 particles were larger than in the presence of other CTFs. Because both peptides were among the strongest inhibitors of Aβ42-induced toxicity, these data suggested a correlation between the inhibition of toxicity and the smaller size of oligomers corresponding to P_1 particles.

The relative abundance of P_1 and P_2 particles showed substantial differences among mixtures of Aβ42 with different CTFs. P_2 particles appeared to be less abundant in the presence of the CTFs that had been found to be effective inhibitors of toxicity (*18*). For example, in the presence of Aβ(30−40), P_2 particles contributed 20% of the scattering on day 2 and 4% on day 7. In contrast, in the presence of Aβ(29−42), which showed weak inhibition of Aβ42-induced toxicity, P_2 particles contributed 74% of the scattering on day 2 and 87% on day 7. Notably, in the presence of Aβ(29−42), the scattering intensity, but not the particle size, grew ~5 times as fast as in all other samples (data not shown), suggesting that aggregates of similar size had larger masses, i.e., were more dense compared to aggregates of Aβ42 alone or in the presence of other CTFs.

In addition to measuring particle size, we also measured the frequency of intensity spikes that occur when large particles cross the laser beam (Figure 3B). This measurement is a convenient proxy of formation of very large particles, presumably fibrils, before they become so large that they precipitate out of solution. Aβ(29−42), Aβ(30−42), Aβ(31−42), and Aβ(30−40) exhibited inhibition of fibril growth relative to Aβ42 in the absence of CTFs or in the presence of the shorter CTFs, Aβ(32−42), Aβ(35−42), and Aβ(39−42).

DISCUSSION

Inhibition of Aβ assembly is an attractive pathway for developing reagents that will block Aβ toxicity and potentially will lead to treatment for AD. Because the assembly process of Aβ is complex and the relationship between assembly size and structure, and toxicity are not well understood, it is important to understand the mechanisms by which inhibitors affect Aβ assembly and how the resulting structures correlate with inhibition of toxicity. Such structure−activity analysis may lead eventually to

the ability to predict factors necessary for successful inhibition of Aβ toxicity.

Here, we used two complementary methods, PICUP and DLS, to study the interaction of peptide inhibitors with Aβ42 and compared the data with our previous characterization of inhibition of Aβ42-induced toxicity by these peptides (*18*) and the biophysical features of the peptides themselves (*19*). The PICUP data showed that Aβ(35−42) and longer CTFs interrupted Aβ42 paranucleus formation, whereas the shorter peptides did not. The order of activity of the CTFs in inhibiting hexamer formation in this assay roughly followed CTF length and did not explain the relatively high potency with which Aβ(30−42), Aβ(31−42), Aβ(39−42), or Aβ(30−40) inhibited Aβ42-induced toxicity.

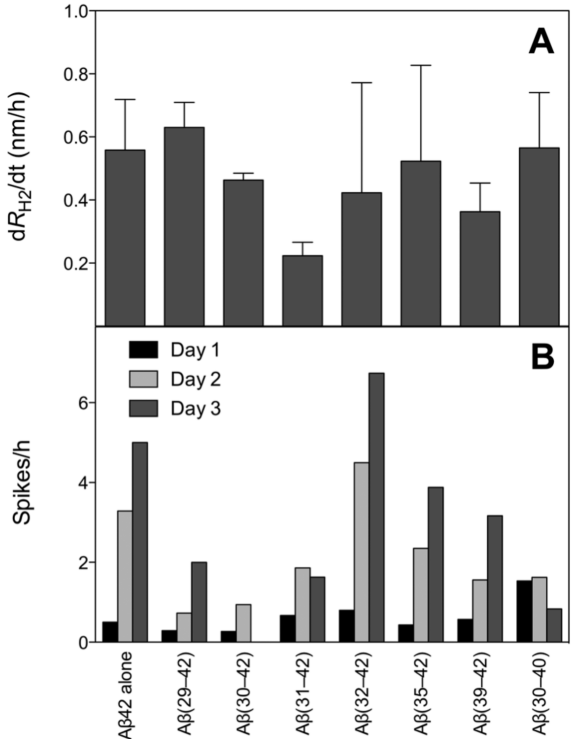

FIGURE 3: DLS monitoring of Aβ42 aggregation in the absence or presence of CTFs. (A) Growth rates (dR_{H2}/dt) of particles with an initial R_{H2} of 20−60 nm. The data for Aβ42 alone could not be obtained consistently (see the text). (B) Intensity spikes per hour indicating fibril development.

DLS measurements showed that CTFs interacted with Aβ42 and stabilized two oligomer populations. The data suggested several lines of correlation between inhibition of Aβ42-induced toxicity and the assembly behavior of different CTFs. The two previously characterized toxicity inhibitors, Aβ(31−42) and Aβ(39−42), exhibited the strongest reduction in the growth rate of P_2 particles, dR_{H2}/dt. However, a slow growth rate alone did not explain the behavior of other CTFs, such as Aβ(30−42) or Aβ(30−40), which showed strong inhibition of Aβ42-induced toxicity but had little effect on dR_{H2}/dt. A decrease in the size of P_1 particles was observed in the presence of Aβ(39−42) or Aβ(30−40), but not other CTFs. Inhibition of formation of putative fibrils measured by the effect of CTFs on the frequency of intensity spikes correlated only partially with inhibition of toxicity and did not provide a satisfactory mechanistic explanation for the toxicity results. These analyses suggested that more than one mechanism might be responsible for inhibition of Aβ42-induced toxicity by CTFs.

To gain additional mechanistic insight, we examined potential sets of correlation among the different data sets, including inhibition of paranucleus formation (Figure 1), abundance of P_2 particles (Figure 2), inhibition of toxicity (ref *18* and Figure S2A of the Supporting Information), CTF solubility (*19*), CTF conversion to β-sheet-rich fibrils (*19*), and CTF particle growth (*19*). We calculated linear correlations among these data sets, which, depending on the parameter and the availability of the data, ranged from four to seven data points. The analysis confirmed a poor correlation between inhibition of paranucleus formation and inhibition of Aβ42-induced neurotoxicity [$r^2 = 0.01$ (Figure 4A)]. Inhibition of paranucleus formation showed a relatively high correlation with CTFs solubility [$r^2 = 0.72$ (Figure 4B)], β-sheet formation [$r^2 = 0.96$ (Figure S3A of the Supporting Information)], and particle size increase [$r^2 = 0.94$ (Figure S3B of the Supporting Information)]. The error bars of the solubility and particle growth rate of the CTFs alone in Figure 4 and Figure S3 are inherently quite large due to the large variability in amyloid peptide samples (*30*). These errors are reflected in the calculated r^2 and p values for the linear correlations. The correlation calculated might raise a concern with regard to precipitation of Aβ42 in the presence of the least soluble CTFs. However, neither SDS−PAGE analysis of cross-linked oligomers (Figure S1 of the Supporting Information) nor the DLS measurements (Figure 2) showed such precipitation or reduced

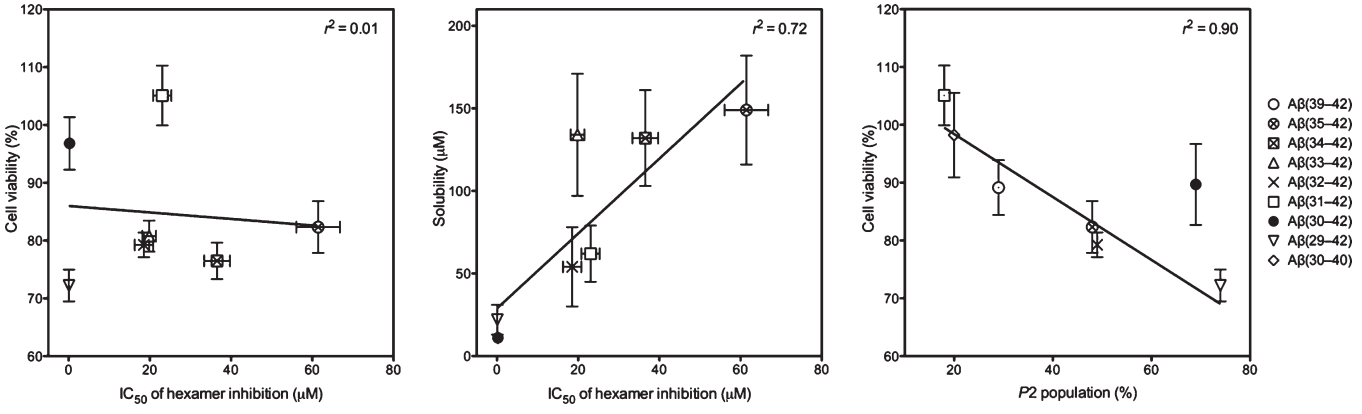

FIGURE 4: Correlation analysis. (A) Linear regression analysis correlating inhibition of paranucleus formation for Aβ(29−42)−Aβ(35−42) with inhibition of Aβ42-induced toxicity (*18*) ($r^2 = 0.01$; $p = 0.8$). (B) Linear regression analysis correlating inhibition of paranucleus formation for Aβ(29−42)−Aβ(35−42) with CTF solubility (*19*) ($r^2 = 0.72$; $p = 0.02$). (C) Linear regression analysis correlating the population of P_2 on day 2 for Aβ(29−42)−Aβ(32−42), Aβ(35−42), Aβ(39−42), and Aβ(30−40) with inhibition of Aβ42-induced toxicity ($r^2 = 0.90$; $p = 0.004$). Aβ(30−40) is an outlier in this correlation, which is not included in the calculation.

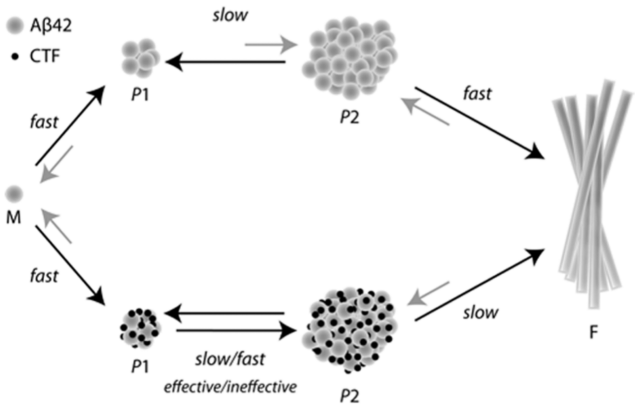

FIGURE 5: Schematic representation of a putative mechanism by which CTFs affect Aβ42 assembly. Monomer (M) assembly into P_1 particles is a fast process in the absence (top path) or presence (bottom path) of CTFs. CTFs may accelerate the conversion of P_1 into P_2 oligomers, but effective inhibitors of Aβ42-induced toxicity induce slower acceleration than ineffective ones, shifting the population toward P_1. All CTFs slow the maturation of P_2 assemblies into fibrils (F).

solubility. Thus, our analysis suggests that the same forces that reduce aqueous solubility and promote fibrillogenesis of CTFs in the absence of Aβ42 also facilitate the interaction of the CTFs with Aβ42, leading to inhibition of paranucleus formation.

Of the different parameters we measured in the DLS experiments (dR_{H2}/dt, the abundance of P_2 particles, and intensity), we found that inhibition of Aβ42-induced toxicity correlated with a low abundance of P_2 particles on day 2 [$r^2 = 0.90$ (Figure 4C)] and on days 4−7 [$r^2 = 0.75$ (data not shown)]. Thus, although the particle distribution initially had an increased contribution of P_2 particles in the presence of all CTFs relative to Aβ42 alone, on subsequent days, the relative contribution of P_2 particles was small for strong inhibitors of toxicity and large for weak inhibitors. For reasons that are not entirely clear, Aβ(30−42) was an outlier and therefore was not included in this analysis.

Though the DLS experiments were conducted under conditions that differ from those of toxicity experiments, the high correlation between the low abundance of P_2 and Aβ42-induced toxicity at 48 h provides important insights into the mechanism(s) by which CTFs might inhibit the toxicity. This putative mechanism is summarized in Figure 5. In the absence of CTFs (Figure 5, top path), Aβ monomers rapidly self-assemble into small oligomers (P_1 particles). Association of these oligomers into larger assemblies (P_2 particles) is relatively slow, whereas the conversion of P_2 assemblies into fibrils or their disassembly back into P_1 oligomers is fast. As a result, little accumulation of P_2 particles is observed. In the presence of CTFs (Figure 5, bottom path), Aβ42 and the CTFs coassemble into heterooligomers. the size of which is generally similar to that of the oligomers formed in the absence of CTFs. The CTFs stabilize both P_1 and P_2 oligomers and retard the conversion of P_2 assemblies into fibrils. However, CTFs vary in their effect on the conversion of the small P_1 oligomers into the larger P_2 oligomers. Effective inhibitors slow this process and give rise to predominantly P_1 oligomers, whereas less effective inhibitors allow for a relatively fast $P_1 \rightarrow P_2$ conversion. Thus, the anticorrelation between P_2 abundance and inhibition of toxicity suggests that a predominant mechanism by which CTFs inhibit Aβ42 toxicity is stabilization of P_1 heterooligomers.

Taken together, our data indicate that CTFs affect Aβ42 assembly in different ways, including disruption of paranucleus formation by Aβ(35−42) and longer Aβ42 CTFs, stabilization of P_1 and P_2 particles by all CTFs, alteration of the size and abundance of P_1 and P_2 assemblies, and coassembly with Aβ42 into heterooligomers. Inhibition of Aβ42 toxicity by CTFs correlates with accumulation of P_1 heterooligomers, suggesting attenuation of $P_1 \rightarrow P_2$ conversion. Stabilization of nontoxic Aβ oligomers is a mechanism shared by other inhibitors of Aβ assembly and toxicity, including *scyllo*-inositol (*31*) and (−)-epigallocatechin gallate (*32*). Thus, we propose that efforts geared toward designing inhibitors of protein self-assembly should focus on diversion of the process toward formation of nontoxic oligomers (or heterooligomers of Aβ and the inhibitor) that can be degraded by cellular clearance mechanisms rather than attempting to prevent monomer self-association.

SUPPORTING INFORMATION AVAILABLE

Figures S1−S3 present examples of PICUP−SDS−PAGE analysis, Aβ(30−40) inhibitory assays, and correlation analysis. This material is available free of charge via the Internet at http://pubs.acs.org.

REFERENCES

1. Prince, M., and Jackson, J., Eds. (2009) Alzheimer's Disease International World Alzheimer Report 2009, Alzheimer's Disease International, London.
2. Hardy, J., and Selkoe, D. J. (2002) The amyloid hypothesis of Alzheimer's disease: Progress and problems on the road to therapeutics. *Science 297*, 353–356.
3. Ferreira, S. T., Vieira, M. N., and De Felice, F. G. (2007) Soluble protein oligomers as emerging toxins in Alzheimer's and other amyloid diseases. *IUBMB Life 59*, 332–345.
4. Dahlgren, K. N., Manelli, A. M., Stine, W. B., Jr., Baker, L. K., Krafft, G. A., and LaDu, M. J. (2002) Oligomeric and fibrillar species of amyloid-β peptides differentially affect neuronal viability. *J. Biol. Chem. 277*, 32046–32053.
5. Roher, A. E., Lowenson, J. D., Clarke, S., Woods, A. S., Cotter, R. J., Gowing, E., and Ball, M. J. (1993) β-Amyloid-(1−42) is a major component of cerebrovascular amyloid deposits: Implications for the pathology of Alzheimer disease. *Proc. Natl. Acad. Sci. U.S.A. 90*, 10836–10840.
6. Bitan, G., Kirkitadze, M. D., Lomakin, A., Vollers, S. S., Benedek, G. B., and Teplow, D. B. (2003) Amyloid β-protein (Aβ) assembly: Aβ40 and Aβ42 oligomerize through distinct pathways. *Proc. Natl. Acad. Sci. U.S.A. 100*, 330–335.
7. Chen, Y.-R., and Glabe, C. G. (2006) Distinct early folding and aggregation properties of Alzheimer amyloid-β peptides Aβ40 and Aβ42: Stable trimer or tetramer formation by Aβ42. *J. Biol. Chem. 281*, 24414–24422.
8. Sciarretta, K. L., Gordon, D. J., and Meredith, S. C. (2006) Peptide-based inhibitors of amyloid assembly. *Methods Enzymol. 413*, 273–312.
9. Hughes, S. R., Goyal, S., Sun, J. E., Gonzalez-DeWhitt, P., Fortes, M. A., Riedel, N. G., and Sahasrabudhe, S. R. (1996) Two-hybrid system as a model to study the interaction of β-amyloid peptide monomers. *Proc. Natl. Acad. Sci. U.S.A. 93*, 2065–2070.
10. Tjernberg, L. O., Naslund, J., Lindqvist, F., Johansson, J., Karlstrom, A. R., Thyberg, J., Terenius, L., and Nordstedt, C. (1996) Arrest of β-amyloid fibril formation by a pentapeptide ligand. *J. Biol. Chem. 271*, 8545–8548.
11. Soto, C., Kindy, M. S., Baumann, M., and Frangione, B. (1996) Inhibition of Alzheimer's amyloidosis by peptides that prevent β-sheet conformation. *Biochem. Biophys. Res. Commun. 226*, 672–680.
12. Lowe, T. L., Strzelec, A., Kiessling, L. L., and Murphy, R. M. (2001) Structure-function relationships for inhibitors of β-amyloid toxicity containing the recognition sequence KLVFF. *Biochemistry 40*, 7882–7889.
13. Pallitto, M. M., Ghanta, J., Heinzelman, P., Kiessling, L. L., and Murphy, R. M. (1999) Recognition sequence design for peptidyl modulators of β-amyloid aggregation and toxicity. *Biochemistry 38*, 3570–3578.
14. Adessi, C., Frossard, M. J., Boissard, C., Fraga, S., Bieler, S., Ruckle, T., Vilbois, F., Robinson, S. M., Mutter, M., Banks, W. A., and Soto,

C. (2003) Pharmacological profiles of peptide drug candidates for the treatment of Alzheimer's disease. *J. Biol. Chem. 278*, 13905–13911.
15. Hughes, E., Burke, R. M., and Doig, A. J. (2000) Inhibition of toxicity in the β-amyloid peptide fragment β-(25−35) using N-methylated derivatives: A general strategy to prevent amyloid formation. *J. Biol. Chem. 275*, 25109–25115.
16. Gordon, D. J., Tappe, R., and Meredith, S. C. (2002) Design and characterization of a membrane permeable N-methyl amino acid-containing peptide that inhibits Aβ1−40 fibrillogenesis. *J. Pept. Res. 60*, 37–55.
17. Pratim Bose, P., Chatterjee, U., Nerelius, C., Govender, T., Norstrom, T., Gogoll, A., Sandegren, A., Gothelid, E., Johansson, J., and Arvidsson, P. I. (2009) Poly-N-methylated amyloid β-peptide (Aβ) C-terminal fragments reduce Aβ toxicity in vitro and in *Drosophila melanogaster*. *J. Med. Chem. 52*, 8002–8009.
18. Fradinger, E. A., Monien, B. H., Urbanc, B., Lomakin, A., Tan, M., Li, H., Spring, S. M., Condron, M. M., Cruz, L., Xie, C. W., Benedek, G. B., and Bitan, G. (2008) C-terminal peptides coassemble into Aβ42 oligomers and protect neurons against Aβ42-induced neurotoxicity. *Proc. Natl. Acad. Sci. U.S.A. 105*, 14175–14180.
19. Li, H., Monien, B. H., Fradinger, E. A., Urbanc, B., and Bitan, G. (2010) Biophysical characterization of Aβ42 C-terminal fragments: Inhibitors of Aβ42 neurotoxicity. *Biochemistry 49*, 1259–1267.
20. Lazo, N. D., Grant, M. A., Condron, M. C., Rigby, A. C., and Teplow, D. B. (2005) On the nucleation of amyloid β-protein monomer folding. *Protein Sci. 14*, 1581–1596.
21. Wu, C., Murray, M. M., Bernstein, S. L., Condron, M. M., Bitan, G., Shea, J. E., and Bowers, M. T. (2009) The structure of Aβ42 C-terminal fragments probed by a combined experimental and theoretical study. *J. Mol. Biol. 387*, 492–501.
22. Merrifield, R. B. (1965) Automated synthesis of peptides. *Science 150*, 178–185.
23. Lomakin, A., Chung, D. S., Benedek, G. B., Kirschner, D. A., and Teplow, D. B. (1996) On the nucleation and growth of amyloid β-protein fibrils: Detection of nuclei and quantitation of rate constants. *Proc. Natl. Acad. Sci. U.S.A. 93*, 1125–1129.
24. Condron, M. M., Monien, B. H., and Bitan, G. (2008) Synthesis and purification of highly hydrophobic peptides derived from the C-terminus of amyloid β-protein. *Open Biotechnol. J. 2*, 87–93.
25. Bitan, G., and Teplow, D. B. (2005) Preparation of aggregate-free, low molecular weight amyloid-β for assembly and toxicity assays. *Methods Mol. Biol. 299*, 3–9.
26. Tikhonov, A. N., and Arsenin, V. Y. (1977) Solution of III-Posed Problems, Halsted Press, Washington, DC.
27. Fancy, D. A., and Kodadek, T. (1999) Chemistry for the analysis of protein-protein interactions: Rapid and efficient cross-linking triggered by long wavelength light. *Proc. Natl. Acad. Sci. U.S.A. 96*, 6020–6024.
28. Bitan, G. (2006) Structural study of metastable amyloidogenic protein oligomers by photo-induced cross-linking of unmodified proteins. *Methods Enzymol. 413*, 217–236.
29. Teplow, D. B., Lazo, N. D., Bitan, G., Bernstein, S., Wyttenbach, T., Bowers, M. T., Baumketner, A., Shea, J. E., Urbanc, B., Cruz, L., Borreguero, J., and Stanley, H. E. (2006) Elucidating amyloid β-protein folding and assembly: A multidisciplinary approach. *Acc. Chem. Res. 39*, 635–645.
30. May, P. C., Gitter, B. D., Waters, D. C., Simmons, L. K., Becker, G. W., Small, J. S., and Robison, P. M. (1992) β-Amyloid peptide in vitro toxicity: Lot-to-lot variability. *Neurobiol. Aging 13*, 605–607.
31. McLaurin, J., Golomb, R., Jurewicz, A., Antel, J. P., and Fraser, P. E. (2000) Inositol stereoisomers stabilize an oligomeric aggregate of Alzheimer amyloid β peptide and inhibit Aβ -induced toxicity. *J. Biol. Chem. 275*, 18495–18502.
32. Ehrnhoefer, D. E., Bieschke, J., Boeddrich, A., Herbst, M., Masino, L., Lurz, R., Engemann, S., Pastore, A., and Wanker, E. E. (2008) EGCG redirects amyloidogenic polypeptides into unstructured, off-pathway oligomers. *Nat. Struct. Mol. Biol. 15*, 558–566.